International Journal of Scientific Research and Engineering Development-– Volume 7 Issue 3, May-June 2024
Available at www.ijsred.com

RESEARCH ARTICLE OPEN ACCESS

METAMATERIAL RECONFIGURABLE ANTENNA FOR MULTIBAND LTE, BLUETOOTH AND WI-MAX APPLICATIONS

Mrs. Noorjahan.M[1] , Mathiyazhagan.p[2], Rajkumar.M[3], Jeeva.R[4]

[1]Assistant Professor Electronics & Communication Engineering, Dhanalakshmi Srinivasan Engineering College (Autonomous), Perambalur, Tamil Nadu .

[2]UG - Electronics & Communication Engineering Dhanalakshmi Srinivasan Engineering College (Autonomous), Perambalur, Tamil Nadu.

[3]UG - Electronics & Communication Engineering, Dhanalakshmi Srinivasan Engineering College (Autonomous), Perambalur, Tamil Nadu.

[4]UG - Electronics & Communication Engineering, Dhanalakshmi Srinivasan Engineering College (Autonomous), Perambalur, Tamil Nadu.

Email:m.noorjahanme@gmail.com[1]

Email: rajkumarmohan9629@gmail.com[3]

ABSTRACT:

In this study, we introduce a cutting-edge "Metamaterial Reconfigurable Antenna" enhanced with a PIN diode. This compact 38x28mm² antenna is specifically designed for multiband LTE, Bluetooth, and Wi-MAX applications, offering unprecedented flexibility and performance.The patch's design features an external square metallic strip that emits a magnetic-current loop in the bottom band. By placing a metamaterial structure near the patch's feed line, an additional loop for the higher band is formed. This 38x28mm^2 antenna is suitable for wireless equipment. The high-frequency structure simulator (HFSS) was used for both design and numerical analysis. The lumped circuit model of the antenna is provided, along with a detailed mathematical derivation. This Multi-band antenna is suitable for LTE, Bluetooth and Wi-MAX applications, with frequencies ranging from 2.67 to 3.40GHz, 3.61 to 3.67GHz, and 0.60 to 0.64GHz. Additionally, it demonstrates. Improvements ranged from 0.15 to 3.81 dBi, and 4.27 to 4.63dBi. This study describes a tiny antenna that functions in the LTE, Bluetooth, and Wi-MAX frequency bands and is affected by metamaterials. A patch's layout includes an external square metallic strip that emits a magnetic-current loop within the bottom band. By placing a metamaterial structure near the patch's feed line, an additional loop for the higher band is formed. This 38x28mm^2 antenna is suitable for wireless equipment. The high-frequency structure simulator (HFSS) was used for both design and numerical analysis. The lumped circuit model of the antenna is provided, along with a detailed mathematical derivation. This Multi-band antenna covers frequencies ranging from 2.67 to 3.40GHz, 3.61 to 3.67GHz, and 0.60 to 0.64GHz. is suitable for LTE and Wi-MAX applications. Furthermore, it demonstrates improvements ranging from 0.15 to 3.81 dBi and 4.27 to 4.63ndBi.

INTRODUCTION:

Wireless communication technologies have advanced rapidly, necessitating the use of lightweight, low-profile, high-performance, multi-band, low-frequency band antennas to support the expanding number of service bands. Several communication systems use distinct frequency bands, including GSM-900, GSM-1800, GPS, WLAN at 2.4GHz and 5GHz, and LTE in lower, middle, and upper bands. ISPs and IEEE 802.11a devices employ the U-NII spectrum, which has distinct frequency ranges for low, mid, and high bands. Wi-MAX and Bluetooth employ ISM band frequencies ranging from 2.4 to 2.85GHz, whereas ISPs use 2.3GHz, 2.5GHz, and 3.5GHz.Techniques for improving antenna performance. Metamaterial antennas use metamaterials to increase the performance of tiny antenna systems and provide better performance than regular antennas.Advanced communication systems require metamaterials to improve bandwidth, gain, efficiency, and support lightweight, multi-band, and high data rateapplications. Metamaterial antennas have the potential to be incorporated into future wireless communication systems due to their efficient and ideal performance. Metamaterials possess unique characteristics like negative permeability, double negative characteristics, and negative refractive index. Dual-band

monopole antenna loaded with open complementary split-ring resonators (OCSRRs) covers the Bluetooth andWi-Maxbands for improved performance Antenna array with two 2x2 circularly polarized square slots (CPSS) is designed for the L- and S-band frequencies range of 1 to 4.34 GHz.

Antenna Design and Metamaterial Integration: Overview of the compact antenna design featuring an external square metallic strip and the strategic use of metamaterials. Discussion on the integration of a PIN diode to enhance reconfigurability.

Frequency Bands and Applications: Coverage of frequency bands spanning 2.67 to 3.40 GHz, 3.61 to 3.67 GHz, and 0.60 to 0.64 GHz. Emphasis on the antenna's suitability for LTE, Bluetooth, and Wi-MAX applications.

PIN Diode Integration: Explanation of the role of the PIN diode in enhancing the antenna's performance. Discussion on the variable resistance of the PIN diode and its impact on signal control.

MEASUREMENTAND METHODOLOGY: In the results and discussion section, the study's findings are analyzed, and the performance of different antenna structures both using and without metamaterials and with imperfect antenna ground planes is compared. The effects of integrating the metamaterial structure at various points across the antenna construction are explored as well, as are the radiation patterns and current placement of the antennas.Is measured in millimeters (mm). The 38x28mm^2 metamaterial antenna under display is printed on a 1.6mm thick(t) FR-4 substrate with a relative permittivity of 4.50 and a loss tangent of 0.02. On the back of the item, there are slots on a ground plane (9 x 28 mm2).With a thickness of 0.035 mm and a conductivity of σ=5×8 s/m, copper functions as the antennas' ground plane and The feed line's width is 1.6 mm, and there is a slight variation in the antennas' resonances are significantly affected by the feed line's width. To test the antenna, a 50Ω small coaxial wire is connected to the feeding metal strip. The combined metamaterial The two-ring resonator is combined with a configuration of splits and metal strips to form the structure. A metal strip that resembles a "z-shape" connects the inner ringresonator's top and lower metal bars. On the other hand, the dimensions of a single unit-cell are fixed to 6.5×8.0×1.635 mm3 along the corresponding (x, y, z) axes. The computer simulation technology (HFSS) Microwave Studio electromagnetic simulator tool is used for all designs, simulations, and research.

The findings and discussion section analyzes the results of the study. It compares the performance of different antenna structures with and without metamaterials and faulty antenna ground planes. The section also explores the impact of integrating the metamaterial structure at different positions within the antenna construction. Additionally, it discusses the radiation pattern and current distribution of the antennas.

In the findings and discussion section, the study's findings are analyzed, and the performance of various antenna structures both with and without metamaterials and with defective antenna ground planes is compared. The effects of integrating the metamaterial structure at various points throughout the antenna construction are also examined, as are the radiation pattern and current distribution of the antennas.

Design Equations for Metamaterial Antenna:

Moreover, to achieve low frequency resonance, a patch with a slotted ground is first built. Metamaterial is then added to improve the antenna's performance while reducing antenna size. None the less, the ground's initial design equations for the embedded metamaterial and slots are as follows.

$$M_W \approx M_L \approx \frac{L_S}{5.25} \approx \frac{W_S}{4}$$

$$S_H \approx \frac{L_g}{3} \approx \frac{W_g}{10.67} \approx \frac{S_w}{1.33}$$

The electromagnetic simulation program HFSS tool, which produces the finite integration technique of Maxwell's equations within boundary condition, has been used to investigate and numerically optimize the expected performances of the metamaterial embedded antenna in terms of return loss, gain, S-parameter, and radiation patterns. To analyze the characteristics of the proposed meta material structure for embedded in the antenna structure refection (S11) and transmission (S21) coefficients are extracted to calculate the effective permittivity (εr),permeability (μr), and refractive index (nr).

The Effective Dielectric Constant, $\epsilon_{re} \approx \frac{\epsilon_r+1}{2} + \frac{\epsilon_r-1}{2}\left(1+\frac{12h}{w}\right)^{-0.5}$ (3)

Fringing Length, $\Delta L \approx 0.412\left\{\frac{(\epsilon_{re}+0.30)\left[\frac{w}{h}+0.26\right]}{L\epsilon_{re}-0.258\left[\frac{w}{h}+0.80\right]}\right\}h$ (4)

Fundamental Frequency, $f_1 \approx \frac{C}{2(L+2\Delta L)\sqrt{\epsilon_{re}}}$ (5)

Where ϵ_r is the dielectric constant of FR-4 substrate, ϵ_r=4.40, 'w' is the width of the antenna element and 'h' is the height of the substrate material. The length and width of the antenna element is given by,

Patch Length, $L \approx \frac{\lambda_0}{2\sqrt{\epsilon_r}} - 2\Delta L \approx \frac{c_0}{2f_0\sqrt{\epsilon_r}} - 2\Delta L$ (6)

Patch Width, $w \approx \frac{\lambda_0}{z}\sqrt{\frac{\epsilon_r+1}{2}} \approx \frac{c_0}{2f_0}\sqrt{\frac{\epsilon_r+1}{2}}$ (7)

$V_1 = S_{21} + S_{11}$ (8)

$V_2 = S_{21} - S_{11}$ (9)

$\epsilon_r \approx \frac{2}{jk_0d} \times \frac{(1-V_1)}{(1+V_1)}$

Effective Permittivity, $\varepsilon_r \approx \frac{e}{j\pi fd} \times \left\{\frac{(1-S_{21}-S_{11})}{(1+S_{21}+S_{11})}\right\}$ (10)

$\mu_r \approx \frac{2}{jk_0d} \times \frac{(1-V_2)}{(1+V_2)}$

Effective Permeability, $\mu_r \approx \frac{e}{j\pi fd} \times \left\{\frac{(1-S_{21}+S_{11})}{(1+S_{21}-S_{11})}\right\}$ (11)

$n_r \approx \sqrt{\varepsilon_r\mu_r}$

Refractive Index, $n_r \approx \frac{c}{j\pi fd} \times \sqrt{\left\{\frac{(S_{21}-1)^2-S_{11}^2}{(S_{21}+1)^2-S_{11}^2}\right\}}$ (12)

The meta material's electromagnetic properties are showr in (a) and (b). Transmittance At 3.18 GHz, resonance is detected, and at 3.55 GHz, reflectance. Negative permeability is achieved negative permittivity at two frequency ranges: 1.59 to 2.96GHz and 3.38 to 4.0GHz, and from 2.21 to 4.0GHz to 3.83GHz. Two significant negative frequency bands are displayed by the refractive index: 1.63 to 3.06GHz and 3.09 to 3.85GHz. If permittivity and permeability are both negative, the refractive index will be negative, which may be found between 2.21 and 2.97 GHz and 3.38 and 3.84 GHz, making the structure a left-handed metamaterial at these frequencies At the transmittance resonance point of 3.51GHz, the permittivity, permeability, and refractive index are -17.24, -12.72,and -15.07 respectively (Table 3). The simulated results of the proposed antenna show resonance points at0.65GHz, 3.18GHz, and 3.51GHz with operating bands over specific frequency ranges, while the Resonance spots at 0.63GHz, 3.21GHz, and 3.63GHz are seen in the measured findings with slightly differing bandwidths.

Validation and Measurement Results of Fabricated Antennas:

Measured acquire levels from 0.05 to 2.70 dBi (2.346 to 2.906GHz) and from 2.73 to 4.24 dBi (2.91 to 3.49GHz). Simulated gain ranges from 4.0 to 4.63dBi (2 to 35GHz) and from 2.89 to 4.54 dBi (2.95 to 3.38 GHz). Frequency range: Measured gain frequency range is from 0.8GHz to 4.0GHz.The simulated frequency vary is from 0.5 GHz to 4.0 GHz due to size capabilities. Provide insights into how the integration of the PIN diode was validated through testing, reinforcing its role in enhancing the antenna's Re-configurability .The measurement results provide validation for the simulated data, although slight discrepancies are observed.

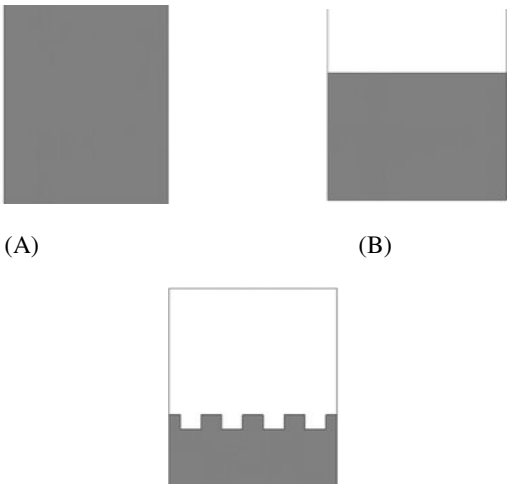

Fig.1(a-c) Existing method Ground plane

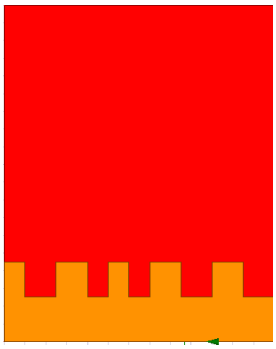

Fig:2 Proposed Method of Ground Plane

Numerical research on antennas with distinctive shapes, how ever barring the embedded metamaterial structure(Ground Plane), are shown in Figure 1(a-c) and the Proposed methos of Ground plane is shown in Fig:2.Antenna-1 exhibits three resonance points covering the L- and S-bands, with respective bandwidths of 30 MHz, 590 MHz, and 430 MHz . This Antenna also has three resonance peaks at 0.91 GHz, 2.15 GHz, and 3.83 GHz, but with smaller bandwidths compared to the antenna-1 configuration. The reduction of strip lines in this antenna configuration leads to a shorter current path and a smaller metallic portion compared to the antenna-1

structure, resulting in variations between these two antenna configurations. It is observed that the high-frequency performance can be improved by employing a square metallic patch near the feed line and PIN diode around the center of the patch (Figure 4(a)) and rearranged metal bar in the antenna structure (Figure 3).

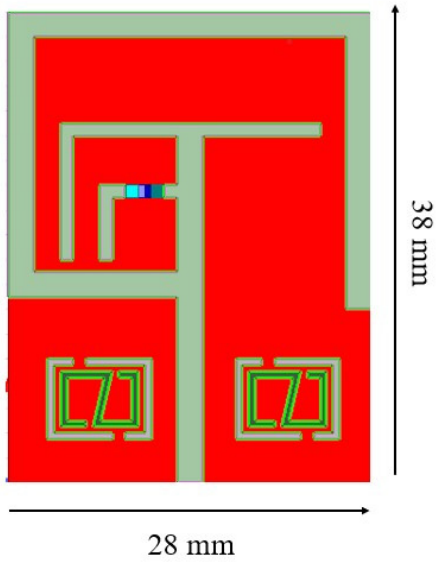

Fig:3 Front View With A Patch Mms Antenna

From these above diagrams of which has represented with Ground plane and patch with PIN Diode, are shown in the fig:2 (Ground plane of proposed method) and fig:3 (Front view of Metamaterial antenna) with the representation of these two figures we can analyze the radiation pattern.

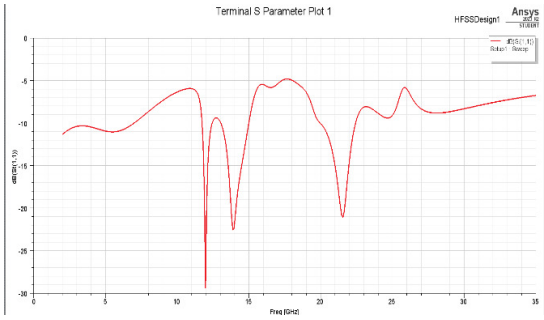

Fig:4

A) S-Parameter Plot

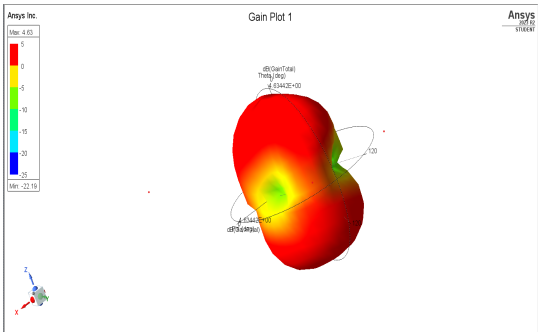

B) Gain Plot

Measured and simulated:

Fig:4 (A) TERMINAL S PARAMETER AND (B) GAIN OF THE METAMATERIAL

Relative permittivity of the substrate influences the discrepancy between measured and simulated findings. Resonant frequency is shifted to a lower frequency via greater permittivity. The measured gains at the Over 2.673.40 GHz and 3.613.67 GHz, there are two working frequency bands: 0.153.81 dBi and 3.473.75 dBi. The measured gain frequencies range from 0.8 GHz to4.0 GHz, but because of the measurement, the simulated frequencies vary from 0.5 GHz to 4.0 GHz. capabilities of Star.The distinctive configurations of the metamaterial-embedded antenna cowl the L- and S-bands with versions in resonant factors and bandwidth.

Metamaterial is an artificial material with unique electromagnetic properties. The distinctive configurations of the metamaterial-embedded antenna cowl the L- and S-bands with versions in resonant factors and bandwidths. Bandwidth is an important parameter indicating how well an antenna can radiate or receive energy across a range of frequencies.

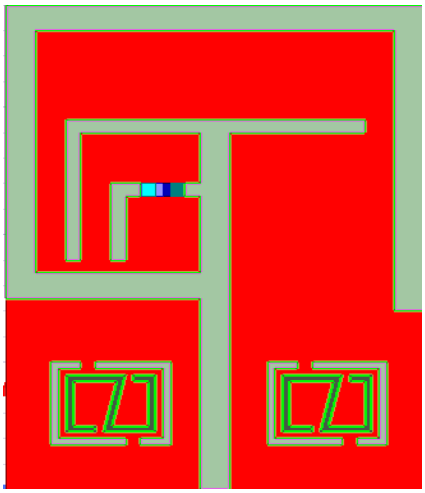

Figure:5

MMs Antenna Confi.1	Resonant Frequency	Band Covered	Bandwidths
MMS Antenna Conf.1	0.65GHz, 3.18GHz, 3.51GHz,	L & S Band	44MHz, 630MHz, 110 MHz
MMS Antenna Conf.2	0.59GHz, 2.89GHz, 3.5 GHz,	L & S Band	36MHz, 330MHz, 267 MHz
MMS Antenna Conf.3	0.60GHz, 2.92GHz, 3.58GHz,	L & S Band	32MHz, 431MHz, 280 MHz

Table:1(a) MMs antenna conf.-1,(b) MMs antenna conf.-2, (c)) MMs antenna conf.-3.

Table:1 Surface Current distribution of the pfthe proposed MMs antenna at**,**

(a)0.63GHz, (b) 3.65GHz and (c)5GHz.

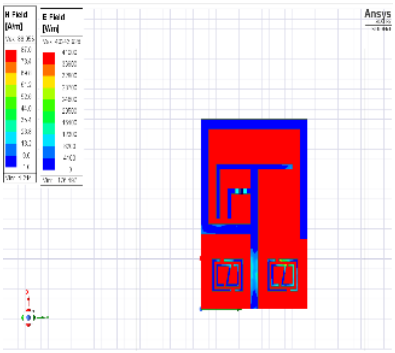

(a)

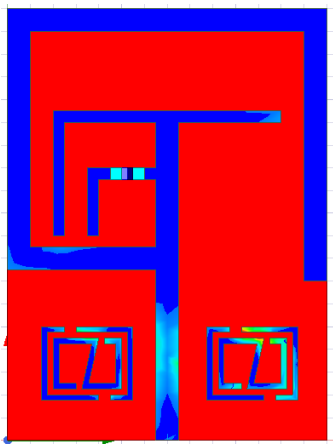

(b)

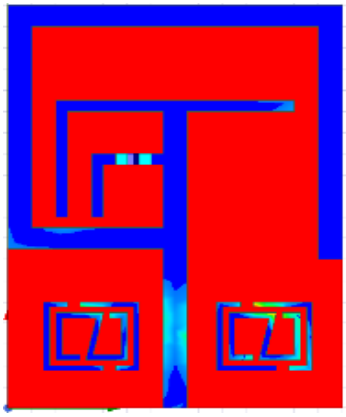

(c)

FIGURE: 6 Performance analysis by integration MMs at different position of the proposed metamaterial antenna

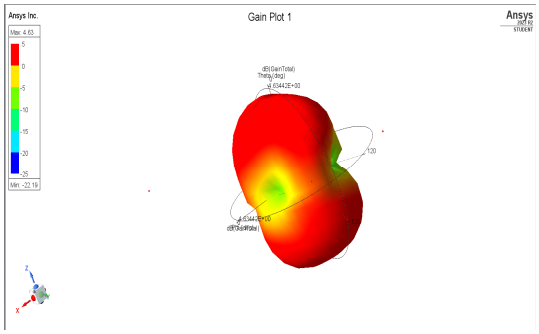

(a)

FIGURE:7 Simulated and Measured radiationpattern of proposed metamaterial inspired antenna at:

(a) 2 - 35GHz.

E-plane (ϕ=0°)

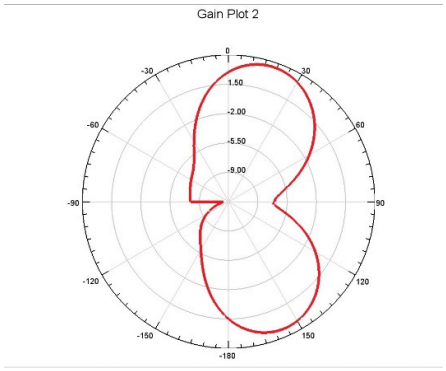

(a)

H-plane(ϕ=90°)

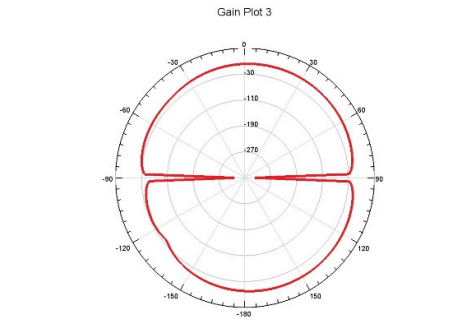

(b)

FIGURE:8 (a ,b) show the comparison between measured and simulated far-field radiation patterns in E-plane and H-plane. The figures are shown from the pattern.

(b) From ϕ=0°(E-plane)andϕ=90° (H-plane).

E-plane (Electric Field Plane):*

- The E-plane of an antenna is defined as the plane perpendicular to the direction of the electric field in the radiation pattern of the antenna.

- In simpler terms, if you visualize the electric field vectors in the radiation pattern of an antenna, the E-plane is the plane that contains these electric field vectors.

- Typically, radiation patterns are plotted in both the E-plane and the H-plane to illustrate how the electromagnetic waves propagate in space.

2. *H-plane (Magnetic Field Plane):*

- The H-plane of an antenna is defined as the plane perpendicular to the direction of the magnetic field in the radiation pattern of the antenna.

- Similarly, if you visualize the magnetic field vectors in the radiation pattern of an antenna, the H-plane is the plane that contains these magnetic field vectors.

- The H-plane is perpendicular to the E-plane.

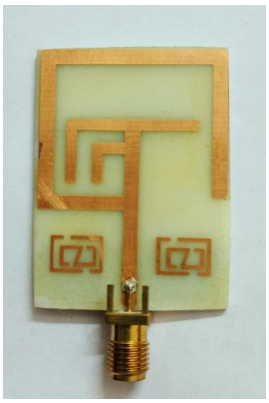

FIGURE:9 Hardware of Metamaterial inspired Reconfigurable antenna

References	Antenna Dimension	Resonant Frequency (GHz)	Covered Bands	Bandwidth (MHz)	Gain (dBi)	Applications
Martínez et al. 3	40 × 30 mm2	2.40, 3.60	S-Band	230, 220	1.4, 1.7	Bluetooth, WiMAX
Li et al. 5	45 × 50 mm2	2.25	S-Band	330	0.97	Bluetooth
Huang et al. 6	45 × 40 mm2	2.40, 5.20	S- and C-Band	1300, 1800 3	3.20, 2.34	WLAN, WiMAX
Bakariya et al. 7	27 × 24 mm2	2.40, 3.50, 5.70	S- and C-Band	85, 400, 125	1.3, 2.5, 3.8	Bluetooth, WLAN, WiMAX
Pushpakaran et al. 8	40 × 38 mm2	2.47, 5.18	S- and C-Band	310, 560	4.5, 7.0	WLAN
Cao et al. 10	44 × 56 mm2	1.54, 2.41, 3.25	L- and S-Band	90, 145, 700	−2, 1.52, 3.0	GPS, WLAN, WiMAX
Zhang et al. 14	115 × 42 mm2	0.90, 1.88	L- and S-Band	376, 1757	0.8, 2.05	GSM
Liu et al. 15	115 × 60 mm	0.85, 1.75	L- and S-Band	271, 1125	2.5, 3.37	GSM, WLAN
Abed et al. 16	70 × 50 mm2	2.45, 3.60	S-Band	260, 350	—	WiFi, WiMAX
Nandi et al. 17	45 × 25 mm2	2.40, 3.50	S-Band	270, 150	−2.0, 0.14	WLAN, WiMAX
Trong et al. 18	88 × 88 mm2	0.9, 1.70	L- and S-Band	40, 120	−0.7, 4.5	GSM
Lee et al. 19	220 × 320 mm2	2.40, 5.20	S- and C-Band	84, 200	6.9, 6.8	WLAN
Chen et al. 20	140 × 75 mm2	0.95	L-Band	262	—	LTE
Proposed MMs Antenna	**38x28 mm^2**	**0.63, 3.21, 3.63**	**L-Band**	**40, 730, 60**	**3.0, 3.69**	**LTE, WiMAX**

TABLE:4 Performance comparison between the proposed MMs antenna with the existing antenna The

content discusses different antennas with varying structures, dimensions, substrate materials, and ground plane designs.

These antennas exhibit identical resonant frequencies but differ in terms of bandwidth, gain, and applications. After a detailed investigation of the existing antennas in Table 5, it is concluded that the proposed metamaterial inspired antenna is compact in size, covers lower frequency bands, has moderate gain, larger bandwidths, and is applicable for LTE and Wi-MAX applications.

Conclusion:

Advancements of wireless communications and electronic warfare systems in new cutting-edge technologies, include metamaterial antennas for leading the improvements in overall system performance A metamaterial inspired on present wireless communication technologies was modified to antenna with covering the L- and S-band frequencies is designed, analyzed and measured in this paper. Discuss other applications of PIN diodes, particularly in the context of RF switching, attenuators, and phase shifters. Simulation results show the metamaterial inspired antenna works well in the lower(0.645~0.689 GHz) and upper (2.75~3.38 GHz) as well as (3.45~3.56 GHz) frequency range. Experimental results are very close to the simulation ones, where the covered lower and upper bands are respectively, (0.60~0.64 GHz), (2.67~3.40 GHz), (3.61~3.67 GHz).The antenna exhibits Omni directional radiation pattern during the operating frequency band with the high peak gain. The antenna can be fabricated easily as well as cheap, simple, and compact for small portable devices. Additionally, the suggested MMs antenna and without MMs antenna have minimal back lobe, high efficiency, consistent radiation properties, and make them excellent candidates for applications like Wi-MAX, Bluetooth, LTE, and others.

REFERENCES ;

1. Hasan, M. M., Faruque, M. R. I., Islam, S. S. & Islam, M. T. A New Compact Double-Negative Miniaturized Metamaterial for Wideband Operation. Materials 9(10), 830 (2016).
2. Hasan, M. M., Faruque, M. R. I. & Islam, M. T. Inverse E-Shape Chiral Metamaterial for Long Distance Telecommunication. Microw. Opt. Technol. Lett. 59, 1772–1776 (2017).
3. Martínez, F. J., Zamora, G., Paredes, F., Martín, F. &Bonache, J. Multiband printed monopole antennas loaded with OCSRRs for PANs and WLANs. IEEE Antennas Wirel. Propag. Lett. 10, 1528–1531 (2011).
4. Pourahmadazar, J. & Rafii, V. Broad Biand circularly polarised slot antenna array for L- and Sband applications. Electron. Lett. 48(10), 542–543 (2012).
5. Li, T., Zhai, H., Wang, X., Li, L. & Liang, C. Frequency-Reconfigurable Bow-Tie Antenna for Bluetooth, WiMAX, and WLAN Applications. IEEE Antennas Wirel. Propag. Lett. 14, 171–174 (2015)
6. Huang, H., Liu, Y., Zhang, S. & Gong, S. Multiband Metamaterial-loaded Monopole Antenna for WLAN/WiMAX Applications. IEEE Antennas Wirel. Propag. Lett. 14, 662–665 (2014)
7. Bakariya, P. S., Dwari, S., Sarkar, M. & Mandal, M. K. Proximity Coupled Microstrip Antenna for Bluetooth, WiMAX and WLAN Applications. IEEE Antennas Wirel. Propag. Lett. 14, 755–758 (2014).
8. Pushpakaran, S. V. et al. A Metaresonator Inspired Dual Band Antenna for Wireless Applications. IEEE Trans. Antennas Propag. 62(4), 2287–2291 (2014).
9. Wong, K. L. & Chen, L. Y. Small-Size LTE/WWAN Tablet Device Antenna with Two Hybrid Feeds. IEEE Trans. Antennas Propag. 62(6), 2926–2934 (2014).
10. Cao, Y. F., Cheung, S. W. & Yuk, T. I. A Multi-bandSlot Antenna for GPS/WiMAX/WLAN Systems. IEEETrans.AntennasPropag. 63(3), 952–958 (2015).
11. Shuai, C. Y. & Wang, G. M. A Novel Planar Printed Dual-Band Magneto-Electric Dipole Antenna. IEEE Access 5, 10062–10067 (2017).
12. Chou, Y. J., Lin, G. S., Chen, J. F., Chen, L. S. & Houng, M. P. Design of GSM/LTE multiband application for mobile phone antennas. Electron. Lett. 51(17), 1304–1306 (2015).
13. Deng, C., Lv, X. & Feng, Z. High Gain Monopole Antenna with Sleeve Ground Plane for WLAN Applications. IEEE Antennas Wirel. Propag. Lett. 16, 2199–2202 (2017).
14. Zhang, T., Li, R. L., Jin, G. P., Wei, G. &Tentzeris, M. M. A Novel Multiband Planar Antenna for GSM/UMTS/LTE/Zigbee/RFID Mobile Devices. IEEE Trans. Antennas Propag. 59(11), 4209– 4213 (2011).
15. Liu, H. J. et al. A Multi-Broad Biand Planar Antenna for GSM/ UMTS/LTE and WLAN/WiMAX Handsets. IEEE Trans. Antennas Propag. 62(5), 2856–2860 (2014).
16. Abed, A. T. & Singh, M. S. J. Slot antenna single layer fed by step impedance strip line for WiFi and Wi-Max applications. Electron. Lett. 52(14), 1196–1198 (2016).
17. Nandi, S. & Mohan, A. CRLH unit cell loaded tri-band compact MIMO antenna for WLAN/WiMAX applications. IEEE Antennas Wirel. Propag. Lett. 16, 1816–1819 (2017).
18. Trong, N. N., Piotrowski, A. &Fumeaux, C. A Frequency-Reconfigurable Dual-Band LowProfile Mono polar Antenna. IEEE Trans. Antennas Propag. 65(7), 3336–3343 (2017).
19. Lee, C. T., Su, S. W., Chen, S. C. & Fu, C. S. Low-Cost, Direct-Fed Slot Antenna Built in Metal Cover of Notebook Computer for 2.4/5.2/5.8-GHz WLAN Operation. IEEE Trans. Antennas Propag. 65(5), 2677–2682 (2017).
20. Chen, H. D., Yang, H. W. & Sim, C. Y. D. Single Open-Slot Antenna for LTE/WWAN Smartphone Application. IEEE Trans. Antennas Propag. 65(8), 4278–4282 (2017).

21. Balanis, C. A. Antenna Theory: Analysis and Design. 3rd Edition. Hoboken. NJ, USA: John Wiley & Sons, Inc. 816–826 (2005).
22. Hasan, M. M., Faruque, M. R. I. & Islam, M. T. Compact Left-Handed Meta-Atom for S-, Cand Ku-Band Application. Appl. Sci. 7(1071), 1–20 (2017).
23. Luukkonen, O., Maslovski, S. I. & Tretyakov, S. A. A stepwise Nicolson–Ross–Weir based material parameter extraction method. IEEE Antennas Wirel. Propag. Lett. 10, 1295–1298 (2011).
24. Clayton, R. P. Inductance: Loop and Partial, New York, NY, USA: Wiley (2009).
25. Hasan, M. M., Faruque, M. R. I. & Islam, M. T. A Mirror Shape Chiral Meta Atom for C-Band Communication. IEEE Access 5, 21217–21222 (2017).

